Research Article
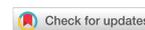
Regional deposited dose in the human respiratory tract using different particulate metrics

Eleftheria Chalvatzaki, Sofia Eirini Chatoutsidou, Mihalis Lazaridis

School of Chemical and Environmental Engineering, Technical University of Crete, Chania 73100, Greece.

Correspondence to: Prof. Mihalis Lazaridis, School of Chemical and Environmental Engineering, Technical University of Crete, Kounoupidiana, Chania 73100, Greece. E-mail: mlazaridis@tuc.gr; lazaridi@mred.tuc.gr

Abstract

The objective of the current study was to calculate the deposited dose rate in the human respiratory tract arising from particle number (PN) and particle mass (PM) measurements. A main objective was the investigation of deposition pattern and characteristics of the two metrics in the human respiratory tract. The dose rate was estimated for residents at a suburban background location (Chania, Greece). The total dose rate showed two peaks, one in the morning (1.6×10^9 particles/h at 7:00-8:00) and the other one at night (2.1×10^9 particles/h at 21:00-22:00), during the warm period, while the cold period showed two peaks, morning (2.0×10^9 particles/h at 9:00-10:00) and afternoon (3.6×10^9 particles/h at 18:00-19:00). The peaks during the warm period were associated with traffic emissions, whereas the peaks during the cold period were associated with both heating and traffic emissions. A higher dose rate of PN_{10} was found in the alveolar region while for PM_{10} it was found in the extrathoracic region. These findings are linked with increased contribution of ultrafine and coarse particles to PN_{10} (65%-78% and 54%-62% for cold and warm periods, respectively) and PM_{10} (63% and 55% for cold and warm periods, respectively) concentrations, respectively. The current study showed the importance to use both number and mass aerosol metrics for determining the human exposure and regional dose and their related health effects. The novelty of the current study is the simultaneous measurements of the two particles metrics and the full particle size distributions to make accurate estimates of regional deposited dose.

Keywords: Dosimetry model, deposited dose, inhaled particles, particle number size distribution, mass concentration

INTRODUCTION

Human exposure to particle number (PN) and particle mass (PM) concentrations has been studied extensively in the scientific literature[1-8]. Investigation of population exposure, especially in urban areas, is important because of the associated health hazard that comes to the residents. Inhalation of airborne particles and the corresponding deposition in the human respiratory tract are directly linked with their concentration. Ambient levels of airborne particles depend on several parameters such as the geographical position, climatological characteristics, urbanization, population density, and anthropogenic activities[7,9-12], as well as different characteristics that accompany the particle size distributions (number *vs.* mass).

Airborne particles can be classified into different size classes (ultrafine, fine, and coarse). Accordingly, fine particles are particles with a diameter less than 2.5 μm, while coarse particles are considered those having diameters ranging from 2.5 to 10 μm. Ultrafine particles are a subset of fine particles, defined as those particles with a diameter less than 100 nm. The main sources of ultrafine and - generally - fine particles are combustion processes such as traffic exhaust, biomass burning, industry, energy production, and aviation[3,13], whereas coarse particles usually originate from soil resuspension, sea spray/salt, and Saharan dust[3,14]. In principle, ultrafine particles are the dominant contributor to the particle number size distribution, whereas the opposite is found when evaluating the particle mass size distribution[2,3,13,15]. The latter is dominated by larger particles due to the significant mass input of coarser particles in the size distribution.

Estimation of the deposited dose of nanoparticles is important due to their ability to penetrate and deposit in the alveolar region, causing significant human health consequences. The increased concern arises for ultrafine particles (< 100 nm) because they are toxic and can cause several adverse health effects on the respiratory and cardiovascular systems such as ischemic heart diseases, oxidative stress, cancer, systemic/pulmonary inflammation, and arrhythmia events[16-18]. Moreover, ultrafine particles are therefore retained longer in the lungs and cause more serious pulmonary inflammation compared to larger particles[19]. Particles in the size range 0.1-1.0 μm are exhaled and, hence, have the lowest total deposition in the human respiratory tract[20]. Coarse particles are responsible for the majority of inflammatory responses to PM_{10}[21].

The regional deposited dose in the human respiratory tract incorporating particle number size distribution data is completely different than that incorporating particle mass size distribution data as a direct consequence of the different inherent characteristics of the two size distributions. Recently, Manigrasso *et al.* found that the highest deposited dose was observed in the extrathoracic (ET) region for PM_{10} while for PN_{10} the highest deposited dose was found in the alveolar-interstitial region[5]. Additionally, Vu *et al.* calculated the dose of traffic-generated particles (13-560 nm) and found that the dose rate of outdoor particles at a traffic site (Bologna, Italy) was 10^{10} particles/h with the majority of particles deposited in the alveolar-interstitial (AI) region[8]. Regarding PM, Chalvatzaki *et al.* found that the deposited mass dose was higher in the ET region, and 75% of the deposited mass dose in the ET region was associated with coarse particles[22]. In addition, Manojkumar and Srimuruganandam found that the deposition of PM_{10} at an outdoor traffic site was higher than that at an outdoor residential site[23]. Therefore, particle deposition in the human respiratory tract is associated with the type of site. A similar finding was observed by Chalvatzaki *et al.*, where the deposited doses of PM_{10} for six major Greek cities were estimated, and they were found to be higher at all urban sites (traffic and urban) compared to suburban background sites[24]. Higher health risks were also obtained for residents in the urban areas. In addition, Gini *et al.* calculated the dose during Saharan dust outbreaks in a suburban site in Athens (Greece) and found that the deposited mass dose was higher (80% for ET region and 27% for lungs) during Saharan dust days compared to non-Saharan dust

days[25]. Saharan dust is an important natural source of coarse airborne particles that causes increased deposited dose in the human respiratory tract.

Estimation of the regional deposited dose rate of airborne particles in the human respiratory tract is an important step for understanding the health effects arising from the inhaled particles. In turn, health effects depend on particle deposition within the human respiratory tract. In the current study, the deposited dose rate was calculated for two particles metrics (mass and number). The simulations were performed on an adult male in a suburban background location. In addition, the study focused on estimating the effect of different characteristics (age, gender, and activity level) of the exposed subject on the deposited dose rate.

MATERIAL AND METHODS

Study area and field measurements

Field measurements were performed at the Akrotiri monitoring station, which is located within the campus of the Technical University of Crete (Chania, Greece). The station is approximately 5 km from the city center of Chania with the surrounding area characterized by medium traffic and consists of a mixed area with agricultural land/farms and low-density residential areas[12,26]. Therefore, the study area is considered a suburban background site with a significant input from the marine environment due to its proximity to the coastline (2 km).

A Scanning Mobility Particle Sizer (SMPS 3938, TSI) consisting of an Electrostatic Classifier 3082 (TSI), a long Differential Mobility Analyzer 3081 (TSI), and a Condensation Particle Counter 3775 (TSI), was used for measuring the particle number size distribution of fine particles. The instrument was operated with aerosol sample flow rate at 0.3 lpm and sheath flow rate at 3 lpm, with the midpoint particle mobility diameter ranging from 13.1 to 661.2 nm (110 size channels). In addition, an Optical Particle Sizer 3330 (OPS, TSI) was used for measuring the particle number size distribution from 0.3 to 10 μm in 16 discrete size channels.

Measurement of the particle mass concentration was performed through a portable aerosol particulate monitor (Dust Trak 8530 EP, TSI) using a PM_{10} pre-head, while an Andersen Cascade Impactor (ACI) was used for obtaining the particle mass size distribution. ACI collected size-segregated particle mass fractions into nine size intervals: four size fractions for fine particles ($PM_{2.1}$) and five size fractions for coarse particles ($PM_{2.1-10}$). Two sampling campaigns were performed: During the first (Campaign I), the particle number size distribution of fine particles was measured throughout a warm period and a cold period. During the second (Campaign II), a full size distribution was obtained by simultaneous measurements of the particle number size distribution (PNSD) with the SMPS and the OPS [Supplementary Figure 1]. In addition to the PNSD measurements, the particle mass concentration and size distribution were measured again throughout a warm period and a cold period. A detailed description of the sampling periods of each campaign is shown in Table 1. In total, the sampling period corresponds to 57 days (32 days for the warm period and 24 days for the cold period) during Campaign I, while, during Campaign II, field measurements were performed for 27 days (13 for the cold period and 14 for the warm period). Field measurements of the particle mass size distribution were performed for six days (four samplings during the cold period and two samplings during the warm period, Supplementary Figure 2).

Dosimetry model

Exposure Dose Model (ExDoM2) is a dosimetry model developed to incorporate ambient particulate concentrations in order to determine the deposited dose rate of the inhaled particles[27]. Simulations can be conducted using freely the particle mass or number measurements depending on the available dataset. In

Table 1. Instruments and sampling periods at Akrotiri station

	Instrument	Sampling period
Campaign I	SMPS	20/08/20 -10/10/20 02/11/20-05/02/ 21
Campaign II	SMPS	24/11/20-30/01/21 24/05/21-09/06/21
	OPS Dust Trak 8530	24/11/20-30/01/21 24/05/21-09/06/21
	Andersen	27/11/20-08/01/21 22-28/05/21

the current study, simulations were performed considering a 24 h exposure in the outdoor environment by assuming a light exercise activity level for an adult male resident.

The deposition module of ExDoM2 is based on the International Commission on Radiological Protection (ICRP) model; therefore, it treats the human respiratory tract as a series of filters[28,29]. Accordingly, the human respiratory tract is divided into nine filters distributed as follows: two in the anterior nose region (ET1); two in the posterior nasal passages, pharynx, and larynx region (ET2); two in the bronchial (BB) region; two in the bronchiolar (bb) region; and one in the AI region. Therefore, the deposition fraction can be sorted within five regions (ET1, ET2, BB, bb, and AI) and estimated as[28]:

$$DE_{ET1} = DE_1 + DE_9 \tag{1}$$

$$DE_{ET2} = DE_2 + DE_8 \tag{2}$$

$$DE_{BB} = DE_3 + DE_7 \tag{3}$$

$$DE_{bb} = DE_4 + DE_6 \tag{4}$$

$$DE_{AI} = DE_5 \tag{5}$$

where DE_1, DE_2, DE_3, and DE_4 are the deposition fractions in the ET1, ET2, BB, and bb filters (inhalation), respectively; DE_5 is the deposition fraction in the AI filter (inhalation and exhalation); and DE_6, DE_7, DE_8, and DE_9 are the deposition fractions in the bb, BB, ET2, and ET1 filters (exhalation), respectively. The deposition fraction in each filter depends on the fraction of tidal air that reaches the j filter (φ_j), the prefiltration efficiency (n_0), and the deposition efficiency of each filter (n_j).

The prefiltration efficiency (n_0) was estimated as[28]:

$$n_0 = 1 - n_I \tag{6}$$

where n_I is the inhalability of particles.

The deposition efficiency (n_j) was calculated by[28]:

$$n_j = (n_{ae}^2 + n_{th}^2)^{1/2} \tag{7}$$

where n_{ae} is the aerodynamic deposition efficiency due to impaction and gravitational settling and n_{th} is the thermodynamic deposition efficiency due to diffusion.

The φ_j during inhalation was calculated by[28]:

$$\varphi_j = 1 \qquad\qquad for\ j = 0 \tag{8}$$

$$\varphi_j = 1 - \frac{1}{V_T} \sum_{jj=0}^{j-1} v_{jj} \qquad\qquad for\ 1 \le j \le \frac{N+1}{2} \tag{9}$$

where V_T is the tidal volume (mL), v_{jj} is the volume of a preceding filter (mL), and N is the number of filters.

The φ_j during exhalation was calculated by [28]:

$$\varphi_j = \varphi_{N-j+1} \qquad\qquad for\ j = \frac{N+3}{2}, N \tag{10}$$

The mobility diameter was converted into the aerodynamic diameter using the following equation[5]:

$$d_{ae} = d_m \sqrt{\frac{\rho\ C(d_m)}{\chi\ C(d_{ae})}} \tag{11}$$

where d_m is the mobility diameter, χ is the shape factor of particles, ρ is the density of particles, $C(d_m)$ is the Cunningham slip correction for a particle of mobility diameter, and $C(d_{ae})$ is the Cunningham slip correction factor for a particle of aerodynamic diameter.

In the present work, the results were classified into three regions: the extrathoracic, tracheobronchial (TB), and alveolar-interstitial regions. The extrathoracic region includes ET1 and ET2, while the TB region includes BB and bb. Finally, a redistribution of 65% to ET1 and 35% to ET2 regions for individual depositions was incorporated, as proposed by ICRP[29].

Clearance
According to ICRP[29], the respiratory tract clearance model consists of 13 compartments. The retained dose of particles in each compartment j and the dose to the esophagus, lymph nodes, and blood was estimated by Equation (12), while Equation (13) was used for rapidly and slowly dissolving particles[22]:

$$\frac{dI_j(t)}{dt} = \sum_{k=1}^{13} \left[m_{k,j} \times I_k(t) - (m_{j,k} + s_r) \times I_j(t) \right] + f_r \times H_j(t) \qquad (12)$$

$$\frac{dT_j(t)}{dt} = \sum_{k=1}^{13} \left[m_{k,j} \times T_k(t) - (m_{j,k} + s_s) \times T_j(t) \right] + (1 - f_r) \times H_j(t) \qquad (13)$$

where $m_{k,j}$ is the mechanical movement rate of particles from compartment k to j; $m_{j,k}$ is the mechanical movement rate of particles from compartment j to k; f_r is the fraction of particles dissolved rapidly; s_r is the rapid dissolution rate; s_s is the slow dissolution rate, H_j is the deposited dose in the compartment j; I_j and I_k are the retained doses of particles dissolving relatively rapidly in the compartment j and k, respectively; and T_j and T_k are the retained doses of particles dissolving slowly in the compartment j and k, respectively. The absorption of particles in the blood was assumed to be moderate. The default values for f_r, s_r, and s_s during moderate absorption were based on ICRP recommendations[29]. Therefore, f_r, s_r, and s_s were set equal to 0.2, 3, and 0.005 d^{-1}, respectively[29].

RESULTS AND DISCUSSION

Diurnal and seasonal variation of deposited number dose rate

The diurnal variations of the deposited dose rate at the Akrotiri station during the warm and cold periods are presented in Figure 1A. The diurnal profile was characterized by two peaks, one in the morning (7:00-8:00) and one at night (21:00-22:00), during the warm period. Specifically, the dose rate was equal to 1.6×10^9 particles/h during the morning peak and 2.1×10^9 particles/h during the night peak. These peaks were associated with traffic and increased vehicular emissions during rush hours. Overall, higher values were obtained during traffic rush hours at night, which is linked with the closing time (21:00) of the commercial stores. It is well known in the scientific literature[8,30,31] that vehicular emissions increase the number concentration of ultrafine particles as well as the corresponding deposited dose. Regarding the cold period, the dose rate in the morning increased after 7:00 with a peak at 9:00-10:00 (2.0×10^9 particles/h), while the second peak was observed at 18:00-19:00 (3.6×10^9 particles/h). It was observed that the afternoon/night peaks were considerably higher than the morning peaks. These peaks were influenced by domestic heating emissions; therefore, increased dose rates were obtained. The opposite characteristic was observed by Vu *et al.*, where the diurnal variation of the number dose rate in Bologna (Italy) showed two peaks with the afternoon peak (16×10^9 particles/h) being lower than the morning peak (22×10^9 particles/h)[8]. According to Aalto *et al.*, the maximum particle number concentrations (between 7 nm and a few micrometers) in five European cities (Augsburg, Barcelona, Helsinki, Rome, and Stockholm) were detected in the morning hours during weekdays, while the opposite characteristic was observed on Sunday, indicating that traffic emissions influence the diurnal behavior[32].

Furthermore, the seasonal comparison showed that the deposited dose during the cold period preserved higher rates compared to the warm period. A similar observation was observed by Voliotis and Samara[33] with cold/warm ratios being equal to 1.2 and 1.6 at the urban traffic and urban background sites in Thessaloniki (Greece), respectively. Domestic heating emissions during the cold period increased the particle number concentrations and the corresponding deposited dose rates. Specifically, the total particle number concentration and dose rate reached 4047 particles/cm^3 and 2.1×10^9 particles/h (21:00-20:00) during the warm period, while the corresponding values during the cold period were 6553 particles/cm^3 and 3.6×10^9 particles/h (18:00-19:00), respectively. It was also characteristic that the deposited dose rate
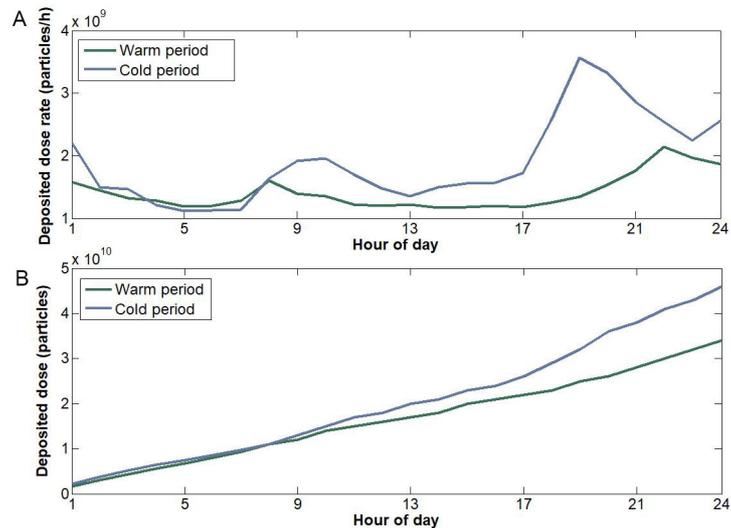
Figure 1. (A) Deposited dose rate (particles/h) and (B) cumulative deposited dose (particles) in the human respiratory tract during warm and cold periods.

followed similar temporal variations with particle concentrations [Supplementary Figure 3]. In the study of Voliotis and Samara[33], the peak dose rate during the cold period was observed at night (21:00-22:00) with a rate of 4×10^{10} particles/h in the urban background site. Intensive wood burning for residential heating purposes was the reason for the high rates, whereas the urban traffic diurnal variations followed traffic flow (9:00, 12:00, and 22:00) with the deposited dose rate during morning peak reaching values close to 7×10^{10} particles/h. Urban anthropogenic activities (traffic emissions and residential heating) are important sources which cause increased deposited dose rates.

The cumulative deposited dose for the warm and cold periods is shown in Figure 1B. A higher cumulative deposited dose was obtained during the cold period (4.6×10^{10} particles/day) in comparison with the warm period (3.4×10^{10} particles/day) as a direct consequence of increased concentration due to the heating emissions. In addition, it was observed that in the early morning hours (1:00-8:00, Figure 1B) the cumulative dose for the two periods was almost equal, as a direct consequence of the similar dose rate obtained for this part of the day [Figure 1A]. Interestingly, the results of this campaign indicate that hourly fine particle number concentrations fluctuate at similar levels after midnight (cold *vs.* warm periods, Supplementary Figure 3), an observation that is influenced by several factors such as the intensity of local sources, temporal variations, and ambient conditions. The daily doses in the current study were close to the results reported by Hussein *et al.*, where the daily deposited dose obtained for submicron particles for an adult male living in Helsinki was found equal to 5.7×10^{10} and 4.0×10^{10} particles/day on workdays and weekends, respectively[34]. In addition, they pointed out that the daily deposited dose would be higher in real-life condition, when indoor sources/activities are also considered.

The deposition fraction in the three regions of the human respiratory for both periods is given in Table 2. A higher deposition fraction was obtained for both cases in the AI region with the deposition fraction being slightly higher during the cold period in comparison with the warm period. Specifically, the deposition in the AI region was equal to 21.7% and 24.2% during the warm and cold periods, respectively. Besides the fact that the deposition fraction did not show important differences between the two periods, the deposited dose rate and the daily deposited dose during the cold period were higher than in the warm period as a direct consequence of higher PN concentrations. Therefore, seasonal variations showed only a slight influence on

Table 2. Average deposition (%) in the three regions (ET, TB, and AI) of the human respiratory tract during warm and cold periods

	ET	TB	AI
Warm period	5.0	5.3	21.7
Cold period	5.3	5.9	24.2

AI: Alveolar-interstitial; ET: extrathoracic; TB: tracheobronchial.

the deposition fraction but had a large effect on the dose rate and daily dose due to differences in PN concentrations. Regarding the other two regions (ET and TB), the deposition was considerably lower (5%-6%). These findings are in agreement with those of Vu *et al.* who found that the majority of particles (number) were deposited in the AI region, with the deposition fraction in the AI region being equal to 0.35 when walking in an outdoor traffic area in Italy[8]. The corresponding values for TB and AI were 0.09 and 0.07, respectively. Finally, a comparison between the two studies revealed that the deposition fraction in AI at the traffic site in Italy[8] was greater than that at this site (suburban background). Therefore, exposure to urban sites with increased traffic results in an increased deposition fraction in the AI region. The increased deposition fraction in AI is associated with health effects. Specifically, deposited particles in AI irritate and corrode the alveolar wall and, hence, cause impaired lung function[35].

Deposition fraction size distribution characteristics
Simulations revealed that the deposition fraction was higher in the AI region for particles in the size range 13-322 nm, while for particles in the size range 334-661 nm the deposition fraction was higher in the ET region [Figure 2]. This finding is linked with the deposition mechanism, especially diffusion, which is the main physical mechanism of particle deposition in AI and its characteristic to increase with decreasing particle size[29,36]. Previous studies have reported that the effect of diffusion is dominant for particles with diameters less than 300-500 nm.

The present results are in agreement with the results reported in previous studies. Particularly, Vu *et al.* found that while walking or cycling the deposition fraction was higher in the AI region for particles with a mobility diameter range of 10-300 nm, while the deposition fraction was higher in the ET region for particles in the 350-560 nm size range[8]. Chalvatzaki and Lazaridis[37] found that the deposition fraction of NaCl without considering the hygroscopicity effect was higher in the AI region for particles with aerodynamic diameters ranging from 15-550 nm, while taking into consideration hygroscopicity the deposition in the AI region was higher for particles in the size range 30-200 nm. This change occurs due to hygroscopic particle growth inside the human respiratory tract.

In addition, it was observed that the highest total deposition fraction occurred for nanoparticles in the lower part of the size distribution (13.1 nm). Patterson *et al.* asserted that the higher total deposition fraction in conjunction with the smaller size causes higher health risk due to the increased possibility to penetrate to the deep lung with more mutagens[38].

Impact of activity level and exposed subject to the dose rate
The impact of the activity level (sitting, light exercise, and heavy exercise) of the exposed subject (adult male) on the deposited dose rate (particles/h) obtained from particle number size distribution data during the cold period is presented in Table 3. It was observed that the deposited dose rate increased with increasing the activity level with the median deposited dose rate increasing from 6.7×10^8 (sitting at rest) to 35.4×10^8 particles/h (heavy exercise). This finding is attributed to the higher inhalation rate [Supplementary Table 1]; the inhalation rates adopted from ICRP[28] for an adult male for heavy exercise, light exercise, and sitting were 3.5, 1.5, and 0.54 m³/h, respectively. The same finding was observed by Daigle *et al.* where the deposited dose of particles (number) in the human respiratory tract was 4.5 times higher

Table 3. Deposited dose rate (median values and confidence interval using student *t*-test distribution) in the human respiratory tract (total) for different activity levels of adult males and for different characteristics (age & gender) of the exposed subject

	Dose rate (× 10^8 particles/h)	Confidence interval (× 10^8 particles/h)	
		Lower	Upper
Adult male			
Sitting	6.7	6.5	8.8
Light exercise	16.7	16.3	21.9
Heavy exercise	35.4	34.4	46.3
Light exercise			
Adult male	16.7	16.3	21.9
Adult female	14.1	13.7	18.5
15-year-old male	14.9	14.5	19.5
15-year-old female	14.3	13.9	18.7
10-year-old	12.1	11.8	15.9
5-year-old	6.3	6.1	8.3
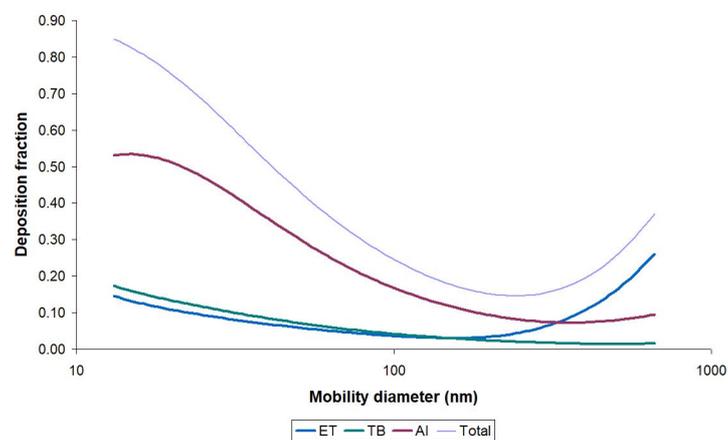
Figure 2. Simulations of fine particle deposition fraction distributions in the respiratory tract of an adult male (light exercise).

during exercise than at rest[39].

To examine the effect of age and gender on the deposited dose rate, the same activity level (light exercise) for all exposed subjects was adopted. Table 3 shows that the median deposited dose rate in the human respiratory tract was higher in adult males (16.7×10^8 particles/h) than in adult females (14.1×10^8 particles/h). Likewise, the deposited dose rate in the human respiratory tract was higher in adult males than in children. These findings are attributed to the higher inhalation rate of an adult male in comparison with an adult female or children. Hussein *et al.* also showed that the deposited dose rate when walking (4 km/h) for sub-micron particles (PN_1) was higher for an adult male (77×10^8 particles/h) than an adult female (67×10^8 particles/h)[40]. In addition, the deposited dose rate was lower in a 5-10-year-old child than in an adult female [Table 2]. However, it is misleading to conclude that adults have a higher health risk than children because children are more vulnerable than adults, and exposure to fine particles early in life may cause long-lasting effects[41]. In addition, a 15-year-old adolescent (male or female) has a higher inhalation rate than an adult female, and hence the median deposited dose rate was higher in the 15-year-old adolescent (14.9×10^8 particles/h for male and 14.3×10^8 particles/h for female) than in the adult female

(14.1×10^8 particles/h). However, the deposited dose rates are more similar between adult females and 15-year-old adolescents than between adult females and adult males. Therefore, the results in Table 3 show that the deposited dose rate varied depending on the age and gender of the exposed subject. However, the current study did not take into consideration different lifestyles (daily activity pattern) between adults and children and as well as between females and males. Specifically, females receive higher doses than males because they spend more time in indoor environments which corresponds to higher exposure levels[1].

Mass and number dose rates

The hourly exposure concentrations ($\mu g/m^3$ or particles/cm^3) and the corresponding deposited dose rates ($\mu g/h$ or particles/h) for PM_{10} and PN_{10} during the cold and warm periods are presented in Figure 3. The results show that the regional deposited dose differed between the two metrics (mass and number). A higher deposited dose rate for PM_{10} was obtained in the ET region (10-22 and 8-10 $\mu g/h$ for cold and warm periods, respectively), while, for PN_{10} the higher deposited dose rate corresponded to the AI region (6×10^8-2×10^9 and 4×10^8-7×10^8 particles/h for cold and warm periods, respectively). These findings are directly linked with the contribution of coarse and ultrafine particles to the particle mass and number size distributions, respectively. Table 4 indicates that coarse particles have negligible contribution to PN_{10} but are the dominant contributor to PM_{10}. The opposite characteristic was observed for ultrafine particles. Supplementary Figures 2 and 4 demonstrate the relative differences between number and mass size distributions. In more detail, the contribution of coarse particles to PM_{10} concentration was equal to 63% for the cold period and 55% for the warm period, whereas the contribution of ultrafine particles (UFPs) to the PN_{10} concentration was equal to 71% ± 3% during the cold period and 59% ± 2% during the warm period. The different regional deposition pattern in the human respiratory tract demonstrates different deposition mechanisms. Specifically, coarse particles are deposited mainly in the ET region due to the impaction mechanism, while ultrafine particles are deposited mainly in AI region due to the diffusion mechanism[28,42]. Additionally, the comparison of mass and number dose indicates differences in the sources between the two metrics. Particles from different sources differ in size as well as in the regional deposition and cause different effects on human health. Specifically, exposure to PN_{10} indicates heating and traffic sources, which cause increased deposited dose in the AI region due to their small size, while exposure to PM_{10} indicates natural sources such as windblown and resuspended dust, which cause increased deposited dose in the ET region due to their large size. This disproportional distribution of regional deposited dose in the human respiratory tract between the two metrics suggests different health implications and highlights the importance of investigating the personal deposited dose on both metrics. Therefore, model results depend strongly on the chosen metric.

It was observed that heating emissions during cold period increased the deposited dose rate for both metrics (PM_{10} and PN_{10}). Specifically, the deposited dose increased by 131% and 59% during the cold period for PN_{10} and PM_{10}, respectively. In addition, the deposited dose rate for both cases (PM_{10} and PN_{10}) in the human respiratory tract (total) was lower in comparison with previous studies[5,43,44]. Manigrasso *et al.* calculated the deposited dose of PM_{10} at an urban background site in Rome and found that the total dose rate ranged from 8.4 to 72 $\mu g/h$ in February while in the current study it ranged from 12-26 $\mu g/h$ during the cold period and 10-13 $\mu g/h$ during the warm period[5]. The urban background site in Rome is close to three roads, and hence higher values were obtained in comparison to the current study. Hussein *et al.* found that the deposited dose rate of PM_{10} was in the range 49-439 $\mu g/h$ for an adult male under different physical exertion levels (e.g., sitting, standing, driving a car, walking, and running) and environments (e.g., urban, rural, and main road) in an eastern Mediterranean city, highlighting the importance of the type of environment for dosimetry calculations[43]. Regarding PN_{10}, Manigrasso *et al.* found that the dose ranged from 2.1×10^9-2.4×10^{10} particles/h in February, while in the current study it ranged from 8.3×10^8-3.6×10^9 particles/h during the cold period and 6.5×10^8-1.0×10^9 particles/h during the warm period[5]. In addition, Buoananno *et al.*

Table 4. Contribution of ultrafine, fine, and coarse particles to the particle mass (PM$_{10}$) and number (PN$_{10}$) size distributions

	Contribution of ultrafine particles	Contribution of fine particles	Contribution of coarse particles
	Cold period		
Mass	6*	37	63
Number**	71 ± 3	100	≈0
	Warm period		
Mass	5*	45	55
Number**	59 ± 2	100	≈0

*The back-up filter of the Andersen impactor, which collects particles less than 0.4 μm. **The results per hour are presented in the Supplementary Materials [Supplementary Figure 4].
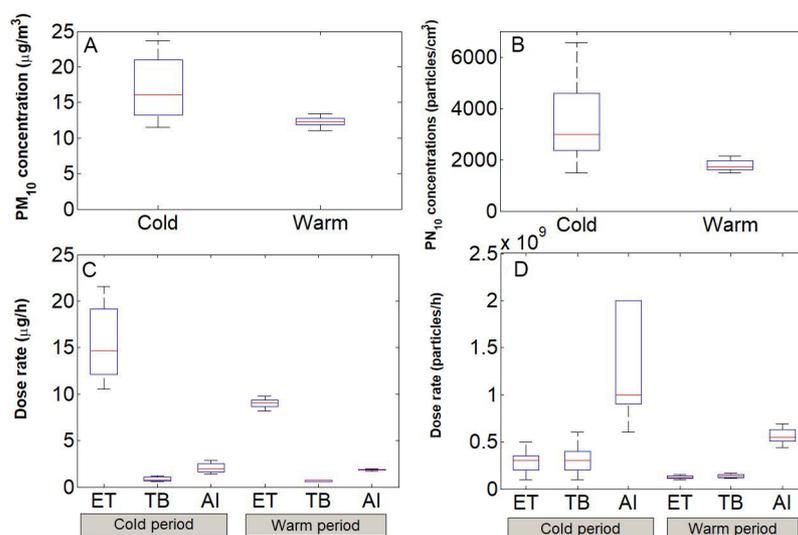

Figure 3. Hourly exposure concentrations of (A) PM$_{10}$ and (B) PN$_{10}$ and the corresponding deposited dose rates based on (C) mass and (D) number metrics during cold and warm periods. AI: Alveolar-interstitial; ET: extrathoracic; PM: particle mass; PN: particle number; TB: tracheobronchial.

calculated the daily dose of sub-micrometer particles for the population in the northern and southern parts of Italy and found that the daily dose in the lungs (TB + AI) was equal to 1.5×10^{11} particles, while in the current study the daily dose of PN$_{10}$ was equal to 4.0×10^{10} and 1.7×10^{10} particles[44]. The higher doses found by Manigrasso *et al.* and Buoananno *et al.* might be attributed to the sampling sites, as measurements were conducted within bigger cities[5,44]. In addition, Buoananno *et al.* considered a daily activity pattern with a high contribution (69%) from the indoor environment (and the associated sources), whereas, in the current study, only the contribution from the outdoor environment was considered[44].

Clearance of deposited PM$_{10}$

Clearance of deposited PM$_{10}$ particles from the human respiratory tract estimated from concentrations of the cold period is presented in Figure 4. Simulations showed that 224 μg were transferred to the esophagus (gastrointestinal tract), 9 μg were absorbed into the blood, 1.1×10^{-4} μg were transferred to the lymph nodes, and 167 μg remained in the respiratory tract (of the total 437 μg deposited to the respiratory tract at the end of the exposure). Thus, the majority of the deposited particles in the human respiratory tract were transferred to the esophagus (51%), a finding that is associated with the high deposited dose in the ET region due to the high contribution of coarse particles to PM$_{10}$. The clearance of PM$_{10}$ depends on the deposition sites: the deposited particles in the ET region are transferred mainly to the GI tract (esophagus)
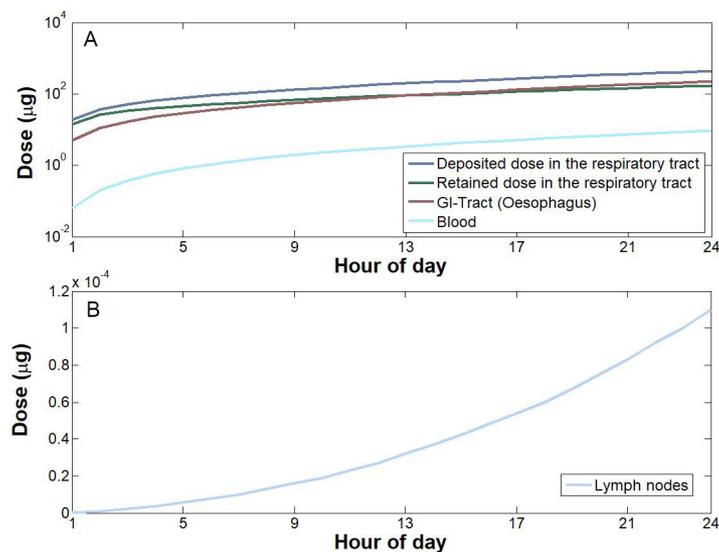
Figure 4. (A) Dose (deposited and retained) in the human respiratory tract, esophagus, and blood; and (B) dose in the lymph nodes.

via mucociliary clearance, while the deposited particles in the TB and AI regions require more time to transfer to the ET2 region and are swallowed to the GI tract, and hence they remain in the respiratory tract and absorbed to the blood[22]. Tomasi *et al.* asserted that mucociliary clearance is a fast process for PM_{10}, while for particles with a diameter less than 3 μm the clearance is less efficient[45]. Thompson *et al.* asserted that 40%-50% of the total mass is retained in the human respiratory tract, which is slightly higher than what was found in the current study (38%)[46]. The present model (ExDoM2) has been used in other studies[22,47] to assess the clearance of PM. Specifically, Chalvatzaki *et al.* applied the model to data from three European cities and found that the dose to the esophagus was equal to 44, 84, and 172 μg for Kuopio, Athens, and Lisbon, respectively[22]. Therefore, the dose to esophagus for all three cities was lower in comparison to the current study. Nevertheless, PM concentrations in Athens (20 μg/m³) and Lisbon (37 μg/m³) were higher than that in the current study (17 μg/m³). The lower dose in the aforementioned cities is linked with the size distribution characteristics; for example, coarse particles corresponded to 63% of the total measured mass concentration in this study, whereas in Athens, Lisbon, and Kuopio they corresponded to 44%, 42%, and 40%, respectively. In addition, Vicente *et al.* applied ExDoM2 and found that the dose to esophagus was equal to 380 and 159 μg for an adult male exposed to wood smoke (indoor) from fireplace and woodstove, respectively, with the corresponding outdoor values being considerably lower (152 and 95 μg, respectively)[47]. This finding is associated with a high risk of developing GI cancer due to indoor biomass burning. Specifically, Sheikh *et al.* found that household biomass burning increased the risk for GI cancer and proposed replacing biomass with natural gas[48]. Therefore, the dose received by a resident during the cold period is significant due to the higher concentration of PM_{10} and the associated increased health effects (increased risk for GI cancer due to transfer of deposited particles to esophagus).

CONCLUSIONS

The dosimetry model ExDoM2 was used to obtain the deposited dose rates of airborne particles in the human respiratory tract in a suburban background site. The novelty of the current study is the combination of concentration and full-size distribution (0.01-10 μm) data for two particle metrics (number and mass), giving a more complete view of human exposure and dose. In turn, the main limitation of the current study is that only the outdoor environment was considered for the calculation of deposited dose, and hence different microenvironments (e.g., home) were not considered during a daily pattern.

Traffic and heating emissions were recognized as significant urban-associated sources that caused an increased deposited dose rate in the human respiratory tract. The activity level, age, and gender of the exposed subjects played significant roles in the calculation of the deposited dose rate. Specifically, the deposited dose rate in the respiratory tract was 1.2 times higher in an adult male than in an adult female. Furthermore, the deposited dose rate was 1.1-2.6 times higher in an adult male than in children, while the deposited dose rate for a 15-year-old male was 1.1 times higher than an adult female. Finally, calculations for three activity levels (sitting, light exercise, and heavy exercise) showed that the deposited dose rate was higher during heavy exercise due to the higher inhalation rate.

Regarding the simultaneous measurements of PM_{10} and PN_{10}, the results show that PM_{10} was deposited mainly in the ET region (cold period, 10-22 μg/h; warm period, 8-10 μg/h) while PN_{10} was deposited mainly in the AI region (cold period, 5.7×10^8-2.5×10^9 particles/h; warm period, 4.4×10^8-6.9×10^8 particles/h). The high deposited dose of PM_{10} in the ET region was associated with a high contribution from coarser particles, whereas the high deposited dose of PN_{10} was associated with a high contribution from ultrafine particles. Overall, simulations demonstrated that seasonal variations and particle origin from variable sources with differences in the size distributions resulted in different regional deposited doses, thus are linked with different health impacts.

DECLARATIONS
Authors' contributions
Conducted model calculations with ExDoM2, performed data analysis and prepared the manuscript: Chalvatzaki E
Performed the field measurements and Review/edit of the manuscript: Chatoutsidou SE
Made substantial contributions to conception, design of the study and review/edit of the manuscript: Lazaridis M
All authors read and approved the final manuscript.

Availability of data and materials
The data is available in the report and supplementary material. Additional data and information can be made available at request from individuals interested.

Conflicts of interest
All authors declared that there are no conflicts of interest.

Ethical approval and consent to participate
Not applicable.

Consent for publication
Not applicable.

Copyright

REFERENCES

1. Buonanno G, Morawska L, Stabile L, Wang L, Giovinco G. A comparison of submicrometer particle dose between Australian and Italian people. *Environ Pollut* 2012;169:183-9. DOI PubMed

2. Buonanno G, Stabile L, Morawska L. Personal exposure to ultrafine particles: the influence of time-activity patterns. *Sci Total Environ* 2014;468-469:903-7. DOI PubMed

3. Harrison RM. Airborne particulate matter. *Philos Trans A Math Phys Eng Sci* 2020;378:20190319. DOI PubMed PMC

4. Manigrasso M, Natale C, Vitali M, Protano C, Avino P. Pedestrians in traffic environments: ultrafine particle respiratory doses. *Int J Environ Res Public Health* 2017;14:288. DOI PubMed PMC

5. Manigrasso M, Costabile F, Liberto LD, et al. Size resolved aerosol respiratory doses in a Mediterranean urban area: From PM_{10} to ultrafine particles. *Environ Int* 2020;141:105714. DOI PubMed

6. Matson U. Indoor and outdoor concentrations of ultrafine particles in some Scandinavian rural and urban areas. *Sci Total Environ* 2005;343:169-76. DOI PubMed

7. Querol X, Alastuey A, Ruiz C, et al. Speciation and origin of PM10 and PM2.5 in selected European cities. *Atmospheric Environment* 2004;38:6547-55. DOI

8. Vu TV, Zauli-sajani S, Poluzzi V, Harrison RM. Factors controlling the lung dose of road traffic-generated sub-micrometre aerosols from outdoor to indoor environments. *Air Qual Atmos Health* 2018;11:615-25. DOI

9. Baek JI, Ban YU. The Impacts of Urban Air Pollution Emission Density on Air Pollutant Concentration Based on a Panel Model. *Sustainability* 2020;12:8401. DOI

10. Rivas I, Beddows DCS, Amato F, et al. Source apportionment of particle number size distribution in urban background and traffic stations in four European cities. *Environ Int* 2020;135:105345. DOI PubMed

11. Rizza V, Stabile L, Buonanno G, Morawska L. Variability of airborne particle metrics in an urban area. *Environ Pollut* 2017;220(Pt A):625-35. DOI PubMed

12. Kopanakis I, Chatoutsidou SE, Glytsos T, Lazaridis M. Impact from local sources and variability of fine particle number concentration in a coastal sub-urban site. *Atmospheric Research* 2018;213:136-48. DOI

13. Chatain M, Alvarez R, Ustache A, Rivière E, Favez O, Pallares C. Simultaneous roadside and urban background measurements of submicron aerosol number concentration and size distribution (in the range 20-800 nm), along with chemical composition in strasbourg, france. *Atmosphere* 2021;12:71. DOI

14. López-caravaca A, Castañer R, Clemente A, et al. The impact of intense winter Saharan dust events on PM and optical properties at urban sites in the southeast of the Iberian Peninsula. *Atmosphere* 2021;12:1469. DOI

15. Rovelli S, Cattaneo A, Borghi F, et al. Mass Concentration and size-distribution of atmospheric particulate matter in an urban environment. *Aerosol Air Qual Res* 2017;17:1142-55. DOI

16. Protano, Vitali, Avino. Nanoparticle behaviour in an urban street canyon at different heights and implications on indoor respiratory doses. *Atmosphere* 2019;10:772. DOI

17. Moreno-ríos AL, Tejeda-benítez LP, Bustillo-lecompte CF. Sources, characteristics, toxicity, and control of ultrafine particles: an overview. *Geoscience Frontiers* 2022;13:101147. DOI

18. Ohlwein S, Kappeler R, Kutlar Joss M, Künzli N, Hoffmann B. Health effects of ultrafine particles: a systematic literature review update of epidemiological evidence. *Int J Public Health* 2019;64:547-59. DOI PubMed

19. Schraufnagel DE. The health effects of ultrafine particles. *Exp Mol Med* 2020;52:311-7. DOI PubMed PMC

20. Brown JS. Chapter 27-deposition of particles. *Compar Bio Normal Lung (Second Edition)* ;2015:513-36. DOI

21. Zwozdziak A, Gini MI, Samek L, Rogula-kozlowska W, Sowka I, Eleftheriadis K. Implications of the aerosol size distribution modal structure of trace and major elements on human exposure, inhaled dose and relevance to the PM2.5 and PM10 metrics in a European pollution hotspot urban area. *J Aeros Sci* 2017;103:38-52. DOI

22. Chalvatzaki E, Chatoutsidou S, Mammi-galani E, et al. Estimation of the personal deposited dose of particulate matter and particle-bound metals using data from selected European cities. *Atmosphere* 2018;9:248. DOI

23. Manojkumar N, Srimuruganandam B. Age-specific and seasonal deposition of outdoor and indoor particulate matter in human respiratory tract. *Atmosp Poll Res* 2022;13:101298. DOI

24. Chalvatzaki E, Chatoutsidou SE, Kopanakis I, et al. Personal deposited dose and its influencing factors at several Greek sites: an analysis in respect to seasonal and diurnal variations. *Environ Sci Pollut Res Int* 2021;28:29276-86. DOI PubMed

25. Gini M, Manousakas M, Karydas AG, Eleftheriadis K. Mass size distributions, composition and dose estimates of particulate matter in Saharan dust outbreaks. *Environ Pollut* 2022;298:118768. DOI PubMed

26. Chatoutsidou SE, Kopanakis I, Lagouvardos K, Mihalopoulos N, Tørseth K, Lazaridis M. PM10 levels at urban, suburban, and background locations in the eastern Mediterranean: local versus regional sources with emphasis on African dust. *Air Qual Atmos Health* 2019;12:1359-71. DOI

27. Chalvatzaki E, Lazaridis M. Development and application of a dosimetry model (ExDoM2) for calculating internal dose of specific particle-bound metals in the human body. *Inhal Toxicol* 2015;27:308-20. DOI PubMed

28.   Human respiratory tract model for radiological protection. A report of a Task Group of the International Commission on Radiological Protection. *Ann ICRP* 1994;24:1-482. PubMed

29.   Paquet F, Etherington G, Bailey MR, et al; ICRP. ICRP publication 130: occupational intakes of radionuclides: part 1. *Ann ICRP* 2015;44:5-188. DOI PubMed

30.   Pant P, Harrison RM. Estimation of the contribution of road traffic emissions to particulate matter concentrations from field measurements: a review. *Atmospheric Environment* 2013;77:78-97. DOI

31.   Rodríguez S, Van Dingenen R, Putaud J, et al. A study on the relationship between mass concentrations, chemistry and number size distribution of urban fine aerosols in Milan, Barcelona and London. *Atmos Chem Phys* 2007;7:2217-32. DOI

32.   Aalto P, Hämeri K, Paatero P, et al. Aerosol particle number concentration measurements in five European cities using TSI-3022 condensation particle counter over a three-year period during health effects of air pollution on susceptible subpopulations. *J Air Waste Manag Assoc* 2005;55:1064-76. DOI PubMed

33.   Voliotis A, Samara C. Submicron particle number doses in the human respiratory tract: implications for urban traffic and background environments. *Environ Sci Pollut Res Int* 2018;25:3372435. DOI PubMed

34.   Hussein T, Löndahl J, Paasonen P, et al. Modeling regional deposited dose of submicron aerosol particles. *Sci Total Environ* 2013;458-460:140-9. DOI PubMed

35.   Xing YF, Xu YH, Shi MH, Lian YX. The impact of PM2.5 on the human respiratory system. *J Thorac Dis* 2016;8:E69-74. DOI PubMed PMC

36.   Hussain M, Pierre M. Lung deposition predictions of airborne particles and the emergence of contemporary diseases Part-I. *the Health* 2011;2:51. Available from: https://biophysics.sbg.ac.at/paper/thehealth [Last accessed on 10 Jun 2022].

37.   Chalvatzaki E, Lazaridis M. A dosimetry model of hygroscopic particle growth in the human respiratory tract. *Air Qual Atmos Health* 2018;11:471-82. DOI

38.   Patterson R. , Zhang Q, Zheng M, Zhu Y. Particle deposition in respiratory tracts of school-aged children. *Aerosol Air Qual Res* 2014;14:64-73. DOI

39.   Daigle CC, Chalupa DC, Gibb FR, et al. Ultrafine particle deposition in humans during rest and exercise. *Inhal Toxicol* 2003;15:539-52. DOI PubMed

40.   Hussein T, Boor BE, Löndahl J. Regional inhaled deposited dose of indoor combustion-generated aerosols in Jordanian urban homes. *Atmosphere* 2020;11:1150. DOI

41.   Oravisjärvi K, Pietikäinen M, Ruuskanen J, Rautio A, Voutilainen A, Keiski RL. Effects of physical activity on the deposition of traffic-related particles into the human lungs in silico. *Sci Total Environ* 2011;409:4511-8. DOI PubMed

42.   Darquenne C. Deposition mechanisms. *J Aerosol Med Pulm Drug Deliv* 2020;33:181-5. DOI PubMed

43.   Hussein T, Saleh S, dos Santos V, Boor B, Koivisto A, Löndahl J. Regional inhaled deposited dose of urban aerosols in an eastern mediterranean city. *Atmosphere* 2019;10:530. DOI

44.   Buonanno G, Giovinco G, Morawska L, Stabile L. Tracheobronchial and alveolar dose of submicrometer particles for different population age groups in Italy. *Atmospheric Environment* 2011;45:6216-24. DOI

45.   Tomasi C, Fuzzi S, Kokhanovsky A. Atmospheric aerosols: Life cycles and effects on air quality and climate. Wiley-VCH. Verlag Gmbh & Co. KGaA, Boschstr. 12, 64469 Weinheim, Germany; 2017, pp704. Available from: https://books.google.com.hk/books?hl=zh-CN&lr=&id=5bCGDQAAQBAJ&oi=fnd&pg=PR15&dq=Tomasi+C,+Fuzzi+S,+Kokhanovsky+A.+Atmospheric+aerosols:+Life+cycles+and+effects+on+air+quality+and+climate.+Wiley-VCH.+Verlag+Gmbh+%26+Co.+KGaA,+Boschstr.+12,+64469+Weinheim,+Germany%3B+2017,+pp704.&ots=SahqgPxYSZ&sig=2FnOVk9HNYNrNQuSmkyRuZVuaJA&redir_esc=y#v=onepage&q&f=false [Last accessed on 10 Jun 2022].

46.   Thompson JE. Airborne particulate matter: human exposure and health effects. *J Occup Environ Med* 2018;60:392-423. DOI PubMed

47.   Vicente ED, Alves CA, Martins V, Almeida SM, Lazaridis M. Lung-deposited dose of particulate matter from residential exposure to smoke from wood burning. *Environ Sci Pollut Res Int* 2021;28:65385-98. DOI PubMed

48.   Sheikh M, Poustchi H, Pourshams A, et al. Household fuel use and the risk of gastrointestinal cancers: the Golestan cohort study. *Environ Health Perspect* 2020;128:67002. DOI PubMed PMC